Benchmark solutions for scattering problems in acoustics

Bernhard Schwarz-Röhr

Universität Oldenburg, D26111 Oldenburg, Germany, Email: bernhard@aku.physik.uni-oldenburg.de

Introduction

Numerical solutions for scattering in acoustics are usually obtained by methods of finite element or boundary element type. Being quite versatile on the hand, these methods do not provide estimates for the accuracy of the solution. Thus analytical solutions for sophisticated testcases are of major importance.

Consider a hollow sphere with thin, rigid walls and an opening linking the inner and outer space. As sketched in fig. 1 a plane wave p_e irradiates the sphere creating a scattered field p_s and a field inside the sphere p_i. The radius of the sphere is denoted by r_0, the angle of the opening by δ. For simplicity the wave vector of the incoming wave is chosen to be in the direction of the symmetry axis of the sphere. The wave number is denoted by k.

The example was chosen on one hand because it combines many critical aspects of computational solutions, namely boundary conditions at infinity for incident and scattered waves as well as resonance effects and coupling for the inner wave. On the other hand analytical solutions including estimates can be found.

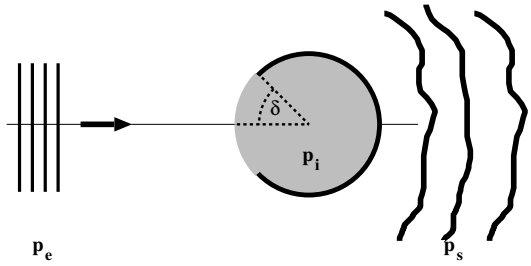

Figure 1: sketch of the problem with the incident wave p_e, the scattered wave p_s and the inner field p_i

Statement of the problem

Introducing spherical co-ordinates r, ϑ, ϕ the solutions of the Helmholtz equation can be expanded into an infinite series

$$p_e = \sum_l a_l \; j_l(kr) \; P_l(\cos(\vartheta)) \tag{1}$$

$$p_s = \sum_l b_l \; h_l(kr) \; P_l(\cos(\vartheta)) \tag{2}$$

$$p_i = \sum_l c_l \; j_l(kr) \; P_l(\cos(\vartheta)). \tag{3}$$

Here a_l, b_l, c_l are the coefficients of the expansion, $j_l(kr)$, $h_l(kr)$ are the spherical Bessel and Hankel functions, P_l denote the Legendre polynomials. Note that any solution given by eqs. 1 to 3 satifies the boundary conditions at infinity automatically.

Hence a solution is found by determining the coefficients b_l and c_l such that the boundary conditions (BC) on the surface are satisfied. Namely the pressure has to be smooth in the opening, leading to

$$p_e(kr_0) + p_s(kr_0) + p_i(kr_0) = 0. \qquad \text{[opening]} \tag{4}$$

$$p'_e(kr_0) + p'_s(kr_0) + p'_i(kr_0) = 0 \qquad \text{[opening]} \tag{5}$$

Here the prime denotes the normal derivative $p'_e = \partial p_e / \partial r$.

Additionally the normal derivative of the outer and inner field has to vanish on the wall,

$$p'_s(kr_0) + p'_e(kr_0) = 0 \qquad \text{[wall]} \tag{6}$$

$$p'_i(kr_0) = 0 \qquad \text{[wall]} \tag{7}$$

Note that due to eq. 7 the eqs. (5), (6) can be combined to read

$$p'_e + p'_s + p'_i = 0 \qquad \text{[everywhere]} \tag{8}$$

So the aim of this paper is to find solutions to eqs. (4), (7) and (8).

Variational formulation

Solutions were sought by minimizing the target functions

$$H := \int_{\text{wall}} dS \;\; |p'_i|^2 \tag{9}$$

$$G := \int_{\text{opening}} dS \;\; |p_e + p_s - p_i|^2 \tag{10}$$

together with eq. 8. Attempting to find simultaneous minima of H and G leads to conflicting linear constraints. So the minimum of $H + \alpha\, G$ with the weight factor α were determined. A sample solution is shown in fig. 2. The accuracy of the solution is checked easily by plotting the surface pressure and velocity (fig. 3). The pressure BC (eq. 4) is satisfied very well. Inner and outer velocity are equal on the whole surface, the velocity vanishes reasonably well on the wall.

Good solutions were found for a broad range of parameters, $8 < kr_0 < 30$ and $10° < \theta < 170°$. Two phenomena were observed, firstly the solution degrades gradually with decreasing kr_0 for $kr_0 < 8$. Secondly there are certain critical values of kr_0 with a comparatively poor solution. In both cases increasing the number of terms in eqs. 1 to 3 does not improve –actually not change– the solution.

Accuracy and stability

Two conditions control the accuracy of the solution. Firstly the incindent wave has to be well approximated by the truncated series eq. 1 on the surface of the scatterer. A well known rule states that the series may be truncated at $l_{max} \gg kr_0$. Secondly l_{max} has to be chosen such that the geometry of the boundary conditions is properly sampled by the Legendre polynomials. The number of Legendre polynomials required is therefore independent of k, in the examples given here an l_{max} of approx. 30 proved sufficient to ensure good solutions.

The behaviour of the solutions is understood from properties of the Bessel ($j_l(\rho)$) and Neumann ($n_l(\rho)$) functions, the latter being the real part of the Hankel functions. Due to the singularity in the Bessel differential equation the Bessel functions start like ρ^l, the Neumann functions have a pole of order $\rho^{-(l+1)}$ (fig. 4) for $\rho \ll \sqrt{l(l+1)}$.

While decreasing the wavenumber for fixed values of l_{max}, the very small contributions of j_l compete with the very large contributions of n_l in the system matrix. This explains the deterioration of the solutions for small wavenumbers. Increasing l_{max} beyond a certain limit does not improve the solution, since adding Bessel functions of high order creates a small contribution compared to those of lower order, see fig. 4. A reconditioning scheme might improve the solutions in both cases but no stable scheme was found yet.

Modal solutions

In fig. 5 a sample solution of a modal approach is shown. In this approach eq. 10 was expanded into the eigenmodes of the homogeneous eq. 9. Compared to the direct solution of fig. 3 the modal approach gives better results for the velocities while the pressure condition is not satisfied very well. The reason is that regardless of l_{max} only a limited number of eigenmodes was found due to the properties of the bessel functions as discussed above. With a proper reconditioning scheme the modal solutions appear to be most promising for future work.

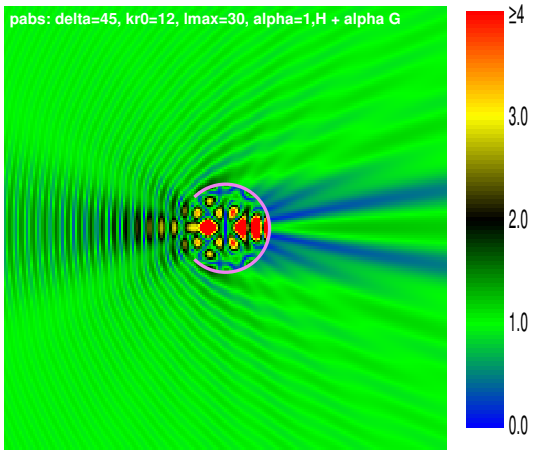

Figure 2: magnitude of the sample solution for kr_0=12, δ=45°, $l_{max} = 30$, $\alpha = 1$

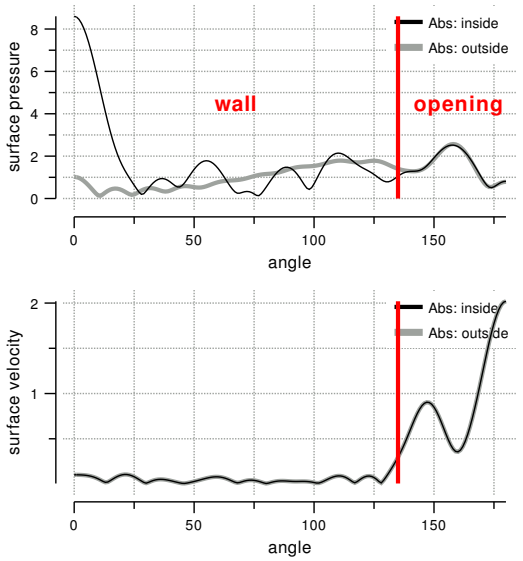

Figure 3: surface values for the sample solution of fig. 2

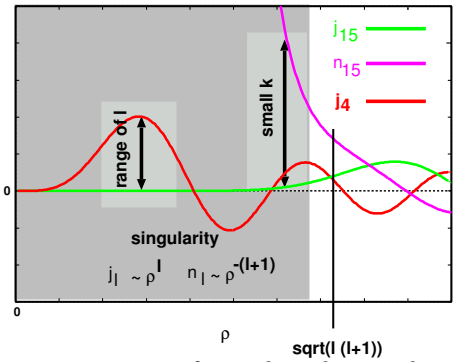

Figure 4: properties of j_l and n_l close to the origin.

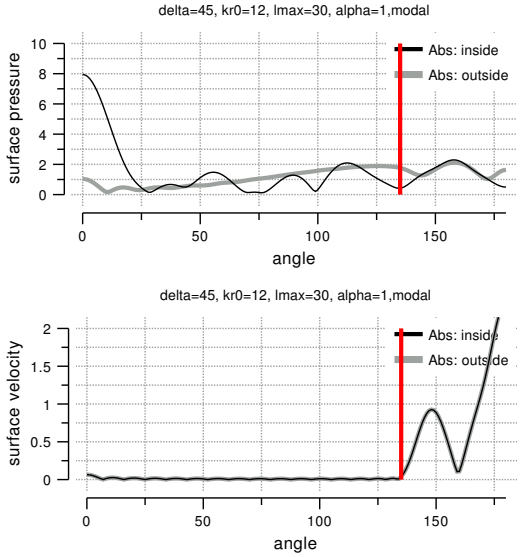

Figure 5: modal solution for the example of fig. 2.

Summary

Solutions for the scattering problem were found for a broad range of parameters. The limits of the algorithm were traced back to the properties of the Bessel and Hankel functions, a reconditioning scheme might be derived from this. Since the accuracy of the solutions is easily checked by analyzing the surface field, the algorithm provides a good tool to benchmark numerical codes.